Materials and Design 188 (2020) 108470

Contents lists available at ScienceDirect

Materials and Design

journal homepage: www.elsevier.com/locate/matdes

Three-dimensional fractal structure with double negative and density-near-zero properties on a subwavelength scale

Yu Liu [a,b], Wenshuai Xu [a,b], Meng Chen [a,b,*], Tao Yang [a,b], Kaijie Wang [c], Xiao Huang [d], Heng Jiang [a,b,*], Yuren Wang [a,b]

[a] Key Laboratory of Microgravity, Institute of Mechanics, Chinese Academy of Sciences, Beijing 100190, China
[b] School of Engineering Science, University of Chinese Academy of Sciences, Beijing 100049, China
[c] Beijing Tongren Eye Center, Beijing Tongren Hospital, Capital Medical University, Beijing Ophthalmology & Visual Sciences Key Lab, Beijing, China
[d] Institute of Applied Physics and Computational Mathematics, Beijing 10094, China

HIGHLIGHTS

- The 3D fractal space-coiling structure has high symmetry and can extend from 2D space to 3D space easily.
- Achieving double negative property and density-near-zero property on a subwavelength scale.
- Excellent acoustic phenomena such as negative refraction and quarter bending transmission.

GRAPHICAL ABSTRACT

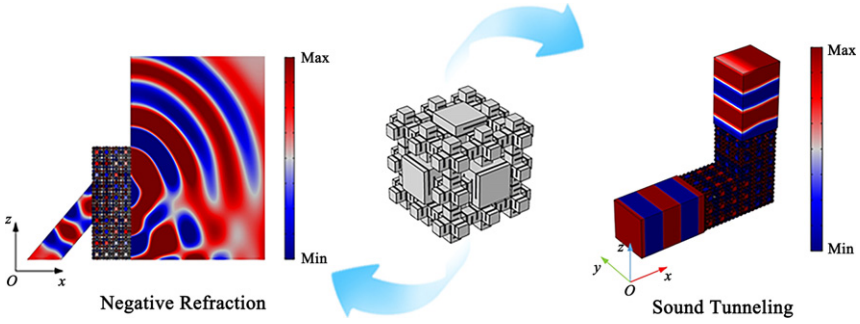

ARTICLE INFO

Article history:
Received 23 November 2019
Received in revised form 1 January 2020
Accepted 2 January 2020
Available online 3 January 2020

Keywords:
3D fractal structure
Negative refraction
Density-near-zero property
Subwavelength scale

ABSTRACT

We constructed a three-dimensional fractal acoustic metamaterial using the combination of zigzag channels and Menger fractal structures that had high structural symmetry and could extend into 3D space easily. Reflection and transmission coefficients were numerically calculated and experimentally measured, and the results matched well with each other. Using the finite element method and the S-parameter retrieval method, the band structures, the equivalent frequency surface and the effective parameters of the acoustic metamaterial were calculated. The results showed that the 3D acoustic metamaterial had double negative property in the normalized frequency range of 0.205–0.269 and density-near-zero property in the normalized frequency vicinity of 0.356. A plate lens model and a quarter-bending model were constructed to demonstrate the double negative property and the density-near-zero property of the acoustic metamaterial, respectively. These results showed that the 3D acoustic metamaterial could achieve excellent acoustic properties and would be promising to construct the 3D double negative structure and control acoustic waves on a subwavelength scale within a single unit.

1. Introduction

Metamaterials are artificial composite materials, own extraordinary physical properties such as negative refraction [1,2] and perfect lens [3,4], and are beyond those readily available in nature. This kind of

* Corresponding authors at: Key Laboratory of Microgravity, Institute of Mechanics, Chinese Academy of Sciences, Beijing 100190, China.
E-mail addresses: chenmeng@imech.ac.cn (M. Chen), hengjiang@imech.ac.cn (H. Jiang).

https://doi.org/10.1016/j.matdes.2020.108470

materials have aroused great interests among researchers and demonstrated huge potential in many exciting applications. In the last ten years, metamaterials have been applied to the most diverse areas, including antennas [5,6], couplers [7,8], filters [9,10], cloaks [11,12], artificial black holes [13,14], tunneling [15,16] and super-resolution imaging [17,18].

In acoustics, control of sound waves on a subwavelength scale was difficult because of the limitations of the mass law until the development of acoustic metamaterials [19–23]. Artificially engineered acoustic metamaterials can not only break the mass law, but also can produce some excellent and unusual acoustic properties, including negative refraction [23–28], acoustic focusing [29–32], and extraordinary transmission [33–34], and have thus attracted the interest of many scientists and researchers. To date, there are several possible ways to design acoustic metamaterials, which are mainly based on locally resonant mechanisms [19–30] and space-coiling mechanisms [31–47]. With regard to the locally resonant mechanism, in 2000, Liu et al. first constructed a locally resonant metamaterial and achieved control of acoustic waves on a subwavelength scale [19]. Lee et al. designed a double negative acoustic metamaterial through introduction of a periodic arrangement of Helmholtz resonators [21]. Yang et al. proposed membrane metamaterials to enable control of low-frequency waves [22]. However, these locally resonant metamaterials can only control waves at their resonant frequency, which causes high losses and leads to narrow operating bandwidths. Furthermore, to achieve the double negative property in locally resonant metamaterials, it is necessary to combine structures with a negative mass density and a negative bulk modulus, which causes construction difficulties and poor structural robustness [29–30], thus limiting the engineering application of these materials.

Unlike the locally resonant mechanism, metamaterials that are designed based on space-coiling mechanisms can achieve excellent acoustic properties and broadband control of acoustic waves within a single unit; these materials have labyrinthine structures and high refractive indexes when compared with that of the background medium. Liang et al. first reported space-coiling acoustic metamaterials with extreme acoustic parameters [34]. Liu et al. proposed an ultra-sparse metasurface based on Mie resonance units for high-level reflection of low-frequency sound [39]. Fu et al. designed a 3D space-coiling metamaterial with both negative mass density and negative bulk modulus [44]. However, it is noteworthy that space-coiling metamaterials with a double negative property have been restricted to simple 2D structures to date [34,39] and there have been no reports on 3D space-coiling fractal metamaterials with a double negative property. Furthermore, the structures of the 3D space-coiling fractal metamaterials reported to date are complex and make construction of these metamaterials difficult [44–47]. Therefore, it will be important to develop an easier method to construct 3D space-coiling fractal structures with extreme acoustic properties.

To date, the 3D metamaterials still exists some problems, which have limited their application in engineering. Aiming at these problems, we adopt an easier way to construct the 3D space-coiling fractal structure through the combining of Menger fractal structure with zigzag channels, and our study has two outweighing strengths: The new designed 3D fractal structure can not only extend easily into 3D space easily, but also have greater symmetry, thus effectively reducing the difficulty of material construction. Furthermore, the new designed 3D fractal structure can also achieve sound tunneling property and double negative property simultaneously with a single unit on a subwavelength scale. This work could be helpful in reducing the construction difficulty and provide a promising way to construct the 3D double negative structure with a single unit on a subwavelength scale (Supplementary Materials).

1.1. Design of the 3D space-coiling fractal structure

Space-coiling structures can achieve extreme acoustic properties with a single unit, however, the way to coil up space straightly into 3D space are complex, causing the difficult construction of 3D space-coiling structure. As known, the Menger fractal structure involves extension of the Sierpinski blanket into 3D space and provides a better way to extend structures from 2D space into 3D space. Furthermore, the Menger structure has high symmetry and multiple resonant modes, making it not only easy to construct, but also with excellent acoustic properties such as double negative and sound tunneling within a single unit. Zigzag channels provide a classical way to coil up space; using this approach, we can effectively extend the transmission routes of the sound waves and construct a structure with a high relative refractive index, which is helpful in controlling acoustic waves on a subwavelength scale. In this study, to simplify the material structure and achieve the desired extreme acoustic properties, we attempt to construct a 3D space-coiling fractal structure by combining the Menger fractal structure with zigzag channels to form a structure that has high symmetry and offers extreme acoustic properties on a subwavelength scale within a single structural unit.

The design process is shown in detail in Fig. 1. Fig. 1(a) shows a schematic diagram of the zigzag channels (height **d**), where identical plates (height $\mathbf{L} = 3/4\mathbf{d}$ and thickness **t**) are embedded into the channel, which can effectively extend the transmission routes of fluids. Fig. 1 (b) shows the acoustic tunnels of the Menger fractal structure (lattice constant $\mathbf{a = 72\ mm}$), in which there are two different sound channel sizes (with height $\mathbf{d_1 = a/3}$ and height $\mathbf{d_2 = a/9}$), and the sound channels are arranged in a simple manner. By combining the Menger fractal structure with the space-coiling structure, we construct the new 3D space-coiling fractal structure with high structural symmetry and excellent acoustic properties on the subwavelength scale; the structure is illustrated in Fig. 1(c). Fig. 1(d) shows the cross-section of the 3D fractal structure and helpfully shows the inner structure clearly. An experimental sample (radius $\mathbf{r = 49.5\ mm}$) was also fabricated to test the reflection and transmission coefficients of the material using the impedance tube, as shown in Fig. 1(e). When compared with the previously reported 3D space-coiling structure, the newly designed 3D fractal structure is easy to extend from 2D space to 3D space. Furthermore, the structure has high symmetry, which is helpful in reducing the construction difficulty and increasing the robustness of the structure and thus shows promise for engineering applications.

2. Double negative property

To enable further study of the acoustic properties of the new designed 3D fractal structure, the band structures and the equivalent frequency surface (EFS) of the structure were calculated, wave equation in the 3D structure can be expressed as:

$$\nabla\cdot\left(-\frac{1}{\rho_0}\nabla p\right)-\frac{w^2 p}{\rho_0 c_0}=0 \tag{1}$$

Here, p is the air pressure, w is the angular frequency, $\rho_0$is the density of the air, and $c_0$is the speed of sound in the air. Sound-hard boundary conditions are set at the air-solid interfaces, and Floquet-Bloch periodic conditions are applied at the boundaries of the unit cells:

$$\frac{\partial p}{\partial n}=0 \tag{2}$$

$$p(x+a)=p(x)e^{-ka} \tag{3}$$

Here, n is the normal vector of the air-solid interface, and k is the wave vector. In this work, the band structures and the equivalent frequency surface were calculated using the finite element method via COMSOL Multiphysics software. By solving for the eigenfrequencies of the designed structures and the w-k dispersion relationships, we obtain the band structures and the equivalent frequency surface the 3D fractal acoustic metamaterials, which are shown in Fig. 2.

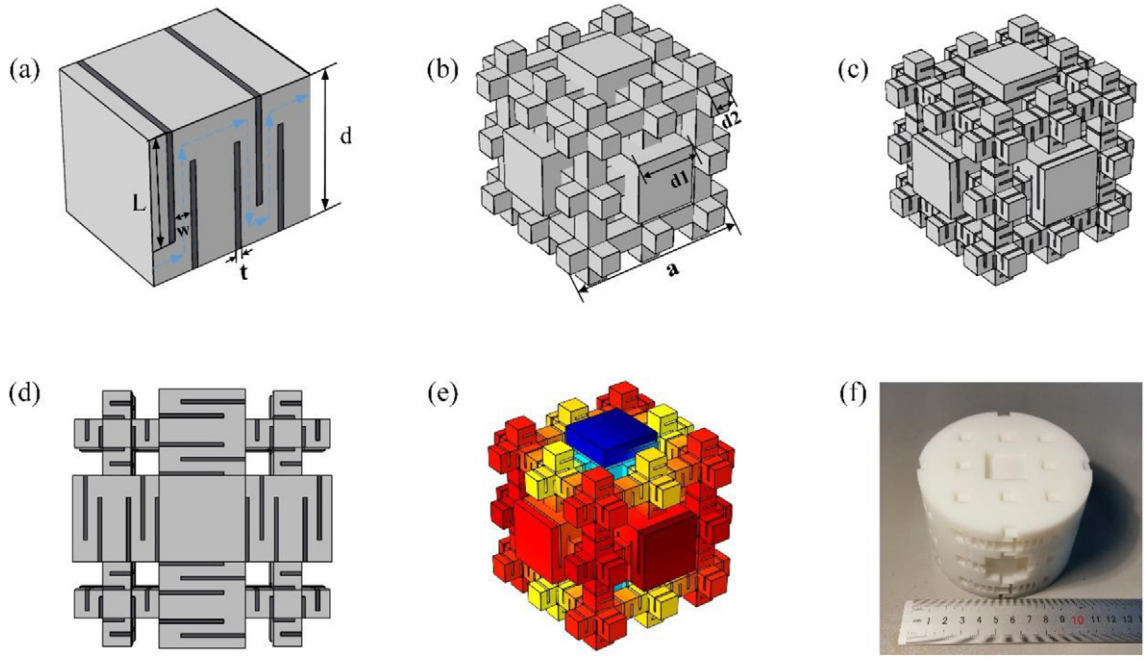

Fig. 1. (a) Schematic diagram of the space-coiling structure. (b) Acoustic tunnels of the Menger fractal structure. (c) Newly designed 3D fractal structure. (d) Cross-section of the 3D fractal structure (e) The eigenmode of the 3D fractal structure (f) Experimental sample of the proposed 3D structure.

Fig. 2(a) shows the band structure results, where the horizontal axis represents the values of the wave vector k along the borders (R–M–Γ–X–R) of the irreducible Brillouin zone of a cubic periodic lattice. In order to show the property of controlling subwavelength scale acoustic waves, we choose the normalized frequency (fa/c_0) in the vertical axis, where f is the frequency, a is the lattice constant and c_0 is the speed of sound in air. There is clearly a negative slope in the second line in the ΓX direction, thus indicating that the newly designed 3D fractal structure has double-negative properties within the normalized frequency range of 0.205–0.269. Furthermore, the normalized frequency is much less than 1, thus proving that the designed 3D fractal structure has a double-negative property on the subwavelength scale.

To study the double-negative property of the designed 3D fractal structure further, the EFS is also calculated and is shown in Fig. 2(b). The EFS result shows that the frequency declines in the ΓX direction, and according to the formulation $\boldsymbol{v_g} = \nabla_{\boldsymbol{k}}\boldsymbol{w}(\boldsymbol{k})$, the gradient direction is in the direction of the group velocities; therefore, the group velocities ($\boldsymbol{S}$) in the 3D fractal structure are oriented in the XΓ direction. However, the wave vector ($\boldsymbol{k}$) is oriented in the ΓX direction, which is in the opposite direction to the group velocities; as a result, $\boldsymbol{S}\cdot\boldsymbol{k} < \boldsymbol{0}$, which further verifies the double-negative property of the proposed 3D fractal structure. In this way, we provide a strong demonstration of the double negative property of the designed 3D fractal structure.

3. Effective parameters

To aid in further understanding of the acoustic properties of the proposed 3D fractal structure, the effective parameters of the structure have also been calculated using the S-parameter retrieval method [48], with results as shown in Fig. 3. The effective mass density and the refractive index of the 3D fractal metamaterial are calculated as follows:

$$\rho_{eff} = \varepsilon \times n \tag{4}$$

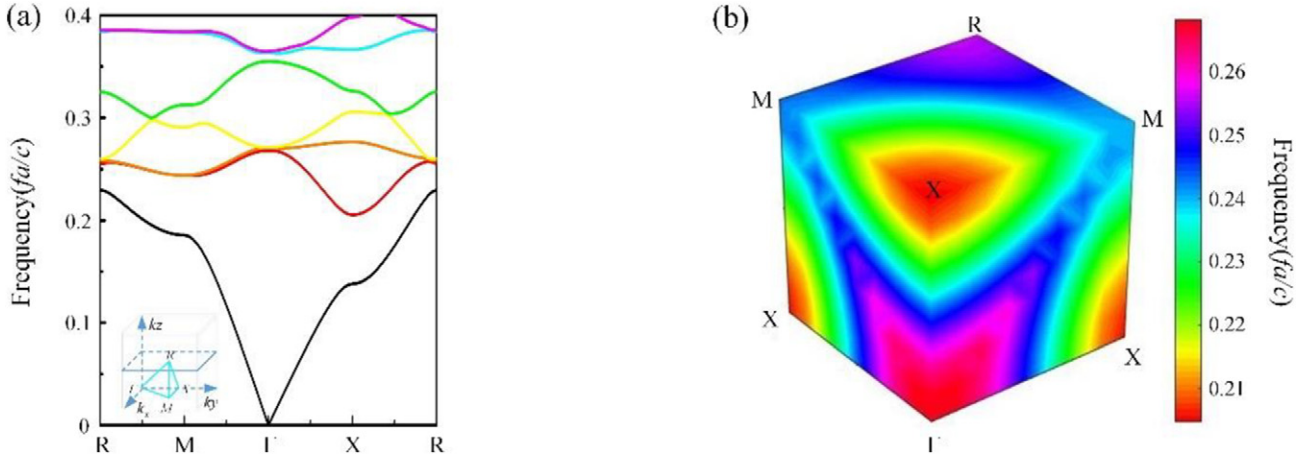

Fig. 2. (a) Band structures of the 3D fractal acoustic metamaterial. (b) EFS of the 3D fractal acoustic metamaterial.

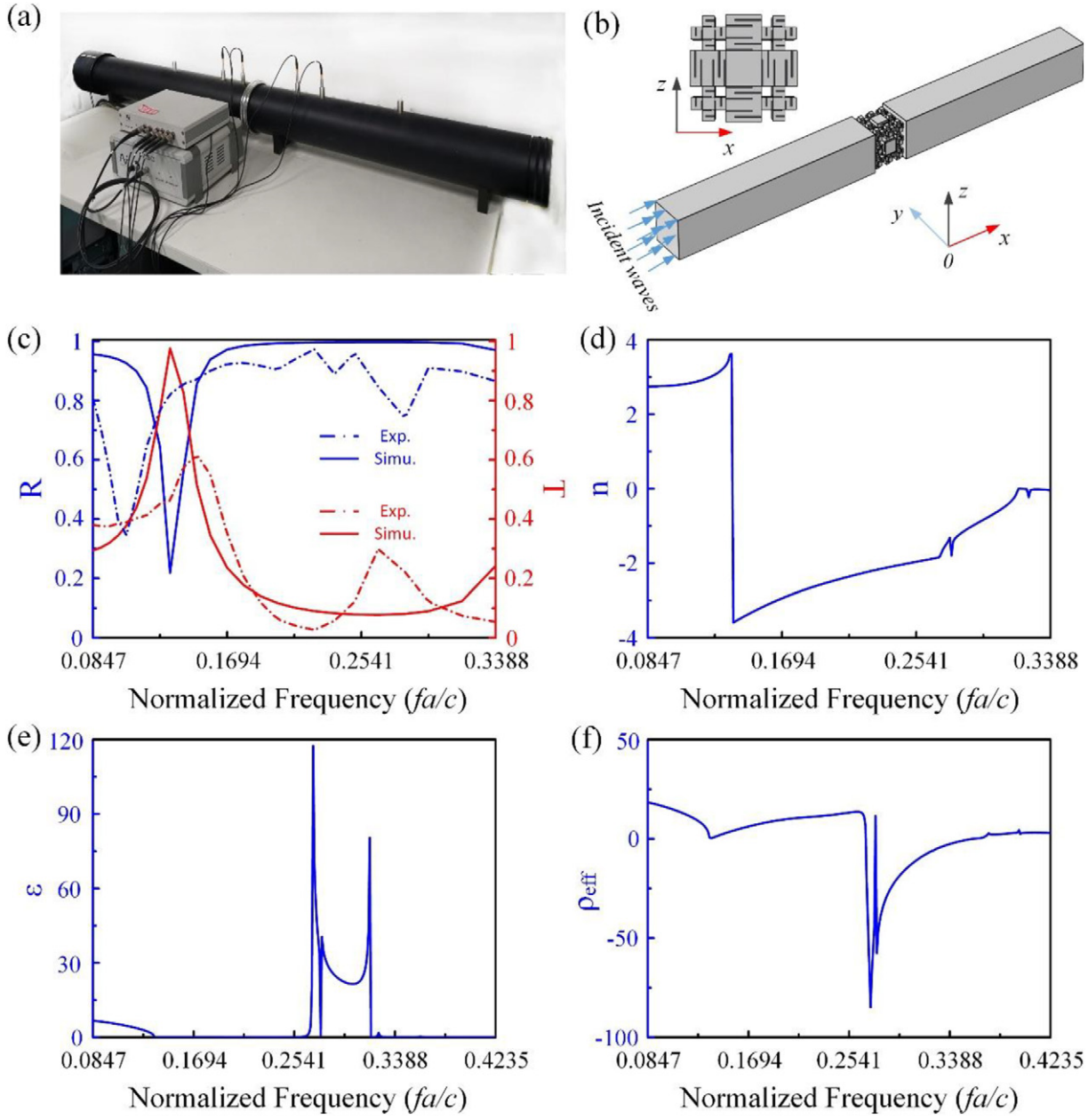

Fig. 3. (a) Experimental setup. (b) Simulation model. (c) Reflection coefficient (R) and transmission coefficient (T). (d) Refractive index. (e) Acoustic impedance. (f) Effective mass density.

$$n = \frac{\pm \cos^{-1}\left(\frac{1}{2T}\left[1-\left(R^2-T^2\right)\right]\right) + 2\pi m}{kd} \tag{5}$$

$$\varepsilon = \pm\sqrt{\frac{(1+R)^2-T^2}{(1-R)^2-T^2}} \tag{6}$$

where $\boldsymbol{\rho_{eff}}$ is the effective mass density, $\boldsymbol{n}$ is the refractive index and $\boldsymbol{\varepsilon}$ is the acoustic impedance.

From the formulation above, we see that the key step required to obtain the effective parameters of the 3D fractal structure is to determine the reflection coefficient (**R**) and the transmission coefficient (**T**). As shown in Fig. 3(c), the reflection coefficient and the transmission coefficient of the 3D structure were calculated via the finite element method using COMSOL Multiphysics software and were also experimentally measured using an impedance tube. In general, the tendencies of the simulated and measured results are well matched, except for the simulated location (**0.2901**) of the peaks being slightly higher than the experimental location (**0.2753**). More importantly, the results agree well with each other within the range from 0.205–0.269, in which the 3D fractal structure has its double-negative property. Furthermore, the matching results also demonstrate the accuracy of the finite element model that we adopted in this work. Because of the limitations of the impedance tube's frequency range, which can only reach a maximum of around 0.33, it cannot meet our measurement requirements. For further study of the acoustic properties of the 3D structure, we therefore calculate the refractive index, the acoustic impedance and the effective mass density using the finite element method, with results as shown in Fig. 3(d), (e) and (f), respectively. These results show that the refractive index is negative within the frequency range from 0.205–0.269, which agrees well with the band structure results, thus further proving the double-negative property. Fig. 3(f) also shows a point in the vicinity of 0.356, which is much smaller than 1, where the effective mass density

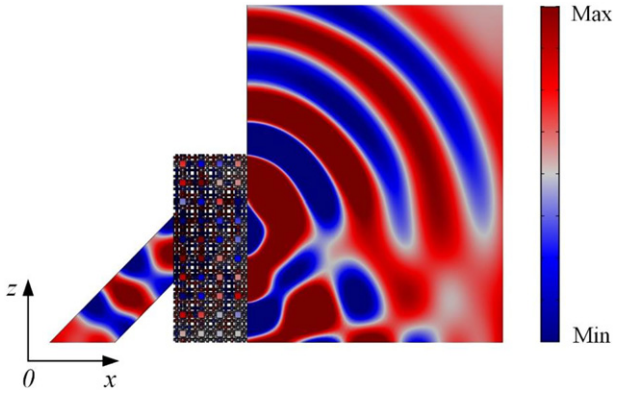

Fig. 4. Sound pressure pattern of an acoustic prism with a 3D fractal structure at a normalized frequency of 0.2647.

is zero. When $\rho_{eff} = 0$, then according to the formulations $c = \sqrt{B/\rho_{eff}}$ and $k = w/c$, the phase velocity c will be infinite and the wave number k will be zero, which indicates that waves can then travel through the 3D fractal structure to achieve a zero phase difference. These results indicate that the 3D fractal structure not only has the double-negative property, but also has a density-near-zero property on the subwavelength scale, which is promising for practical applications.

4. Extreme acoustic properties

The calculation results for the band structure and the effective parameters show that the newly designed fractal structure in this work not only has a double negative property but also has a density-near-zero property, which indicates its promise for applications in engineering. To provide a further demonstration of the 3D fractal structure's double-negative property and density-near-zero property for engineering applications, we choose a plate lens model [49–53] and a quarter-bending model [35]. In the study of the double-negative property, because of the high symmetry of the 3D fractal structure and the calculation limitations of our computer, we simplify the calculations in the *x*-*z* planes and then mainly study the phenomena that occur in the *x*-*z* planes. As shown in Fig. 4, the plate lens has a thickness of 4 units and a height of 10 units, and Gaussian acoustic waves at a normalized frequency of 0.2647 impinge on the lens at an angle of 45°; after passing through the lens, these waves can still be transmitted along their original direction, which strongly indicates the negative-refraction phenomenon in the material and further demonstrates the double-negative property of the 3D fractal structure.

To verify the density-near-zero property, we use a 3D fractal structure containing 81 units to design the quarter-bending model as shown in Fig. 5(a), which represents an acoustic bending waveguide with 90 bends. Plane acoustic waves are incident from the left side and are transmitted along the *x*-direction; when the plane acoustic waves travel through the quarter corner, they turn to be transmitted along the *z*-direction and the outgoing waves in the pattern are still plane waves. For comparison, in Fig. 5(b), the quarter-bending model is constructed using ordinary structures; when acoustic waves pass through these structures, they are strongly scattered and cannot be transmitted in the plane wave pattern, thus providing further proof that the 3D fractal structure has the density-near-zero property.

5. Conclusions

In conclusion, we have constructed a 3D fractal metamaterial with high symmetry by combining a Menger fractal structure with a space-coiling structure. The double-negative property of this structure is demonstrated by calculating the band structures and the EFS. The reflection coefficient and the transmission coefficient of the 3D structure are measured experimentally and calculated numerically and the results agree well with each other. The calculated results for the effective parameters show that the 3D fractal structure not only has the double-negative property in the normalized frequency range of 0.205–0.269, but also has a density-near-zero property in the normalized frequency vicinity of 0.356, which is demonstrated via excellent phenomena such as negative refraction and quarter bending transmission. These results indicate that the newly designed 3D fractal metamaterial has excellent acoustic properties and will be promising for use in engineering applications.

CRediT authorship contribution statement

Yu Liu: Data curation, Formal analysis, Investigation, Methodology, Software, Validation, Writing - original draft. **Wenshuai Xu:** Validation, Software, Investigation, Methodology. **Meng Chen:** Funding acquisition, Formal analysis, Investigation, Writing - review & editing. **Tao Yang:** Validation, Software, Investigation. **Kaijie Wang:** Funding acquisition, Methodology. **Xiao Huang:** Funding acquisition, Methodology. **Heng Jiang:** Funding acquisition, Investigation, Methodology, Writing - review & editing, Project administration. **Yuren Wang:** Funding acquisition, Conceptualization, Project administration.

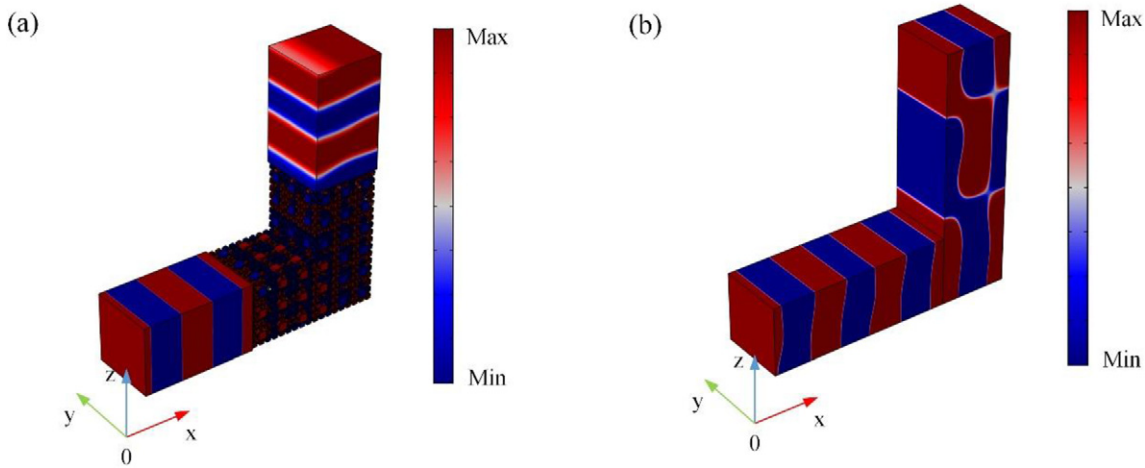

Fig. 5. (a) Sound pressure distribution when acoustic waves propagate through a quarter-bending model with a 3D fractal structure at a normalized frequency of 0.3562. (b) Sound pressure distribution when acoustic waves propagate through a quarter-bending model with an ordinary structure at a normalized frequency of 0.3562.

Declaration of competing interest

The authors declare that there are no conflicts of interest regarding the publication of this article.

Acknowledgement

The authors acknowledge that this project was supported by the National Natural Science Foundation of China (Grant Nos. 11602269, 11602027 and 11802213), the Strategic Priority Research Program of the Chinese Academy of Sciences (Grant No. XDB22040301), the Research Program of Beijing (Grant Nos. Z161100002616034, Z171100000817010 and Z191100002019013) and Beijing Natural Science Foundation (7172056).

Appendix A. Supplementary data

Supplementary data to this article can be found online at https://doi.org/10.1016/j.matdes.2020.108470.

References

[1] D.R. Smith, J.B. Pendry, M.C. Wiltshire, Metamaterials and negative refractive index, Science 305 (5685) (2004) 788–792.
[2] N. Kaina, F. Lemoult, M. Fink, G. Lerosey, Negative refractive index and acoustic superlens from multiple scattering in single negative metamaterials, Nature 525 (7567) (2015) 77.
[3] A.A. Zharov, N.A. Zharova, R.E. Noskov, I.V. Shadrivov, Y.S. Kivshar, Birefringent left-handed metamaterials and perfect lenses for vectorial fields, New J. Phys. 7 (1) (2005) 220.
[4] M. Tsang, D. Psaltis, Magnifying perfect lens and superlens design by coordinate transformation, Phys. Rev. B 77 (3) (2008), 035122.
[5] R. Yahya, A. Nakamura, M. Itami, T.A. Denidni, A novel UWB FSS-based polarization diversity antenna, IEEE Antennas Wirel. Propag. Lett. 16 (2017) 2525–2528.
[6] Y.L. Zhou, X.Y. Cao, J. Gao, S.J. Li, Y.J. Zheng, In-band RCS reduction and gain enhancement of a dual-band PRMS-antenna, IEEE Antennas Wirel. Propag. Lett. 16 (2017) 2716–2720.
[7] H. Qiu, Y. Su, P. Yu, T. Hu, J. Yang, X. Jiang, Compact polarization splitter based on silicon grating-assisted couplers, Opt. Lett. 40 (9) (2015) 1885–1887.
[8] A. Hadij-ElHouati, P. Cheben, A. Ortega-Moñux, J.G. Wangüemert-Pérez, R. Halir, J.H. Schmid, Í. Molina-Fernández, Distributed Bragg deflector coupler for on-chip shaping of optical beams, Opt. Express 27 (23) (2019) 33180–33193.
[9] J. Čtyroký, J. Gonzalo Wangüemert-Pérez, P. Kwiecien, I. Richter, J. Litvik, J.H. Schmid, Í. Molina-Fernández, A. Ortega-Moñux, M. Dado, P. Cheben, Design of narrowband Bragg spectral filters in subwavelength grating metamaterial waveguides, Opt. Express 26 (1) (2018) 179–194.
[10] P. Cheben, J. Čtyroký, J.H. Schmid, S. Wang, J. Lapointe, J.G. Wangüemert-Pérez, Í. Molina-Fernández, A. OrtegaMoñux, R. Halir, D. Melati, D. Xu, S. Janz, M. Dado, Bragg filter bandwidth engineering in subwavelength grating metamaterial waveguides, Opt. Lett. 44 (4) (2019) 1043–1046.
[11] R. Liu, C. Ji, J.J. Mock, J.Y. Chin, T.J. Cui, D.R. Smith, Broadband ground-plane cloak, Science 323 (5912) (2009) 366–369.
[12] H. Chen, B. Zheng, L. Shen, H. Wang, X. Zhang, N.I. Zheludev, B. Zhang, Ray-optics cloaking devices for large objects in incoherent natural light, Nat. Commun. 4 (2013) 2652.
[13] U. Leonhardt, T.G. Philbin, General relativity in electrical engineering, New J. Phys. 8 (10) (2006) 247.
[14] E.E. Narimanov, A.V. Kildishev, Optical black hole: broadband omnidirectional light absorber, Appl. Phys. Lett. 95 (4) (2009), 041106.
[15] R. Liu, Q. Cheng, T. Hand, J.J. Mock, T.J. Cui, S.A. Cummer, D.R. Smith, Experimental demonstration of electromagnetic tunneling through an epsilon-near-zero metamaterial at microwave frequencies, Phys. Rev. Lett. 100 (2) (2008), 023903.
[16] R. Fleury, A. Alù, Extraordinary sound transmission through density-near-zero ultranarrow channels, Phys. Rev. Lett. 111 (5) (2013), 055501.
[17] B.D.F. Casse, W.T. Lu, Y.J. Huang, E. Gultepe, L. Menon, S. Sridhar, Super-resolution imaging using a three-dimensional metamaterials nanolens, Appl. Phys. Lett. 96 (2) (2010), 023114.
[18] X. Yang, J. Yin, G. Yu, L. Peng, N. Wang, Acoustic superlens using Helmholtz-resonator-based metamaterials, Appl. Phys. Lett. 107 (19) (2015), 193505.
[19] Z. Liu, X. Zhang, Y. Mao, Y.Y. Zhu, Z. Yang, C.T. Chan, P. Sheng, Locally resonant sonic materials, Science 289 (2000) 1734–1736.
[20] Y. Pennec, B. Djafari-Rouhani, H. Larabi, J.O. Vasseur, A.C. Hladky-Hennion, Low-frequency gaps in a phononic crystal constituted of cylindrical dots deposited on a thin homogeneous plate, Phys. Rev. B 78 (2008), 104105.
[21] J. Li, C.T. Chan, Double-negative acoustic metamaterial, Phys. Rev. E 70 (2004), 055602.
[22] Z. Yang, J. Mei, M. Yang, N.H. Chan, P. Sheng, Membrane-type acoustic metamaterial with negative dynamic mass, Phys. Rev. Lett. 101 (2008), 204301.
[23] J. Li, X. Zhou, G. Huang, G. Hu, Acoustic metamaterials capable of both sound insulation and energy harvesting, Smart Mater. Struct. 25 (2016), 045013.
[24] S. Nemat-Nasser, Inherent negative refraction on acoustic branch of two dimensional phononic crystals, Mech. Mater. 132 (2019) 1–8.
[25] X. Zhang, Z. Liu, Negative refraction of acoustic waves in two-dimensional phononic crystals, Appl. Phys. Lett. 85 (2004) 341–343.
[26] L. Feng, X.P. Liu, Y.B. Chen, Z.P. Huang, Y.W. Mao, Y.F. Chen, Y.Y. Zhu, Negative refraction of acoustic waves in two-dimensional sonic crystals, Phys. Rev. B 72 (2005), 033108.
[27] A.A. Mokhtari, Y. Lu, A. Srivastava, On the emergence of negative effective density and modulus in 2-phase phononic crystals, J. Mech. Phys. Solids 126 (2019) 256–271.
[28] R. Zhu, X.N. Liu, G.K. Hu, C.T. Sun, G.L. Huang, Negative refraction of elastic waves at the deep-subwavelength scale in a single-phase metamaterial, Nat. Commun. 5 (2014) 5510.
[29] Y. Ding, Z. Liu, C. Qiu, J. Shi, Metamaterial with simultaneously negative bulk modulus and mass density, Phys. Rev. Lett. 99 (9) (2007), 093904.
[30] M. Yang, G. Ma, Z. Yang, P. Sheng, Coupled membranes with doubly negative mass density and bulk modulus, Phys. Rev. Lett. 110 (13) (2013), 134301.
[31] L. Bai, H.Y. Dong, G.Y. Song, Q. Cheng, B. Huang, W.X. Jiang, T.J. Cui, Impedance-matching wavefront-transformation lens based on acoustic metamaterials, Adv. Mater. Technol. 3 (2018), 1800064.
[32] G.Y. Song, B. Huang, H.Y. Dong, Q. Cheng, T.J. Cui, Broadband focusing acoustic lens based on fractal metamaterials, Sci. Rep. 6 (2016) 35929.
[33] Y. Li, B. Liang, X. Tao, X.F. Zhu, X.Y. Zou, J.C. Cheng, Acoustic focusing by coiling up space, Appl. Phys. Lett. 101 (2012), 233508.
[34] Z. Liang, J. Li, Extreme acoustic metamaterial by coiling up space, Phys. Rev. Lett. 108 (2012), 114301.
[35] X. Man, Z. Luo, J. Liu, B. Xia, Hilbert fractal acoustic metamaterials with negative mass density and bulk modulus on subwavelength scale, Mater. Des. 180 (2019), 107911.
[36] J. Liu, L. Li, B. Xia, X. Man, Fractal labyrinthine acoustic metamaterial in planar lattices, Int. J. Solids Struct. 132 (2018) 20–30.
[37] X. Man, T. Liu, B. Xia, Z. Luo, L. Xie, J. Liu, Space-coiling fractal metamaterial with multi-bandgaps on subwavelength scale, J. Sound Vib. 423 (2018) 322–339.
[38] A.O. Krushynska, F. Bosia, M. Miniaci, N.M. Pugno, Spider web-structured labyrinthine acoustic metamaterials for low-frequency sound control, New J. Phys. 19 (2017), 105001.
[39] Y. Cheng, C. Zhou, B.G. Yuan, D.J. Wu, Q. Wei, X.J. Liu, Ultra-sparse metasurface for high reflection of low-frequency sound based on artificial Mie resonances, Nat. Mater. 14 (2015) 1013.
[40] A.O. Krushynska, F. Bosia, N.M. Pugno, Labyrinthine acoustic metamaterials with space-coiling channels for low-frequency sound control, Acta Acustica United with Acustica 104 (2018) 200–210.
[41] M. Miniaci, A. Krushynska, A.S. Gliozzi, N. Kherraz, F. Bosia, N.M. Pugno, Design and fabrication of bioinspired hierarchical dissipative elastic metamaterials, Phys. Rev. Appl. 10 (2018), 024012.
[42] Z. Liang, T. Feng, S. Lok, F. Liu, K.B. Ng, C.H. Chan, J. Li, Space-coiling metamaterials with double negativity and conical dispersion, Sci. Rep. 3 (2013) 1614.
[43] L. Zigoneanu, B.I. Popa, S.A. Cummer, Design and measurements of a broadband two-dimensional acoustic lens, Phys. Rev. B 84 (2011), 024305.
[44] X.F. Fu, G.Y. Li, M.H. Lu, G. Lu, X. Huang, A 3D space coiling metamaterial with isotropic negative acoustic properties, Appl. Phys. Lett. 111 (2017), 251904.
[45] T. Frenzel, J. David Brehm, T. Bückmann, R. Schittny, M. Kadic, M. Wegener, Three-dimensional labyrinthine acoustic metamaterials, Appl. Phys. Lett. 103 (2013), 061907.
[46] C. Zhang, X. Hu, Three-dimensional single-port labyrinthine acoustic metamaterial: perfect absorption with large bandwidth and tunability, Phys. Rev. Appl. 6 (2016), 064025.
[47] X.F. Man, B.Z. Xia, Z. Luo, J. Liu, 3D Hilbert fractal acoustic metamaterials: low-frequency and multi-band sound insulation, J. Phys. D. Appl. Phys. 52 (2019), 195302.
[48] V. Fokin, M. Ambati, C. Sun, X. Zhang, Method for retrieving effective properties of locally resonant acoustic metamaterials, Phys. Rev. B 76 (2007), 144302.
[49] J. Christensen, F.J.G. de Abajo, Anisotropic metamaterials for full control of acoustic waves, Phys. Rev. Lett. 108 (12) (2012), 124301.
[50] M.H. Lu, C. Zhang, L. Feng, J. Zhao, Y.F. Chen, Y.W. Mao, N.B. Ming, Negative birefraction of acoustic waves in a sonic crystal, Nat. Mater. 6 (10) (2007) 744.
[51] V.M. García-Chocano, J. Christensen, J. Sánchez-Dehesa, Negative refraction and energy funneling by hyperbolic materials: an experimental demonstration in acoustics, Phys. Rev. Lett. 112 (14) (2014), 144301.
[52] J. Li, Z. Liu, C. Qiu, Negative refraction imaging of acoustic waves by a two-dimensional three-component phononic crystal, Phys. Rev. B 73 (5) (2006), 054302.
[53] N. Kaina, F. Lemoult, M. Fink, G. Lerosey, Negative refractive index and acoustic superlens from multiple scattering in single negative metamaterials, Nature 525 (7567) (2015) 77.